Correspondence

Comparison of Two Measurement Fusion Methods for Kalman-Filter-Based Multisensor Data Fusion

Currently there exist two commonly used measurement fusion methods for Kalman-filter-based multisensor data fusion. The first (Method I) simply merges the multisensor data through the observation vector of the Kalman filter, whereas the second (Method II) combines the multisensor data based on a minimum-mean-square-error criterion. This paper, based on an analysis of the fused state estimate covariances of the two measurement fusion methods, shows that the two measurement fusion methods are functionally equivalent if the sensors used for data fusion, with different and independent noise characteristics, have identical measurement matrices. Also presented are simulation results on state estimation using the two measurement fusion methods, followed by the analysis of the computational advantages of each method.

I. INTRODUCTION

Consider the following tracking problem. A dynamic target is tracked by N disparate sensors, each with different measurement dynamics and noise characteristics. How can we combine the multisensor measurements to obtain a joint state-vector estimate which is better than the individual sensor-based estimates? There are various multisensor data fusion approaches to resolve this problem, of which Kalman filtering is one of the most significant. Methods for Kalman-filter-based data fusion, including state-vector fusion and measurement fusion, have been widely studied over the last decade [1–10]. As shown in Fig. 1(a), state-vector fusion methods use a group of Kalman filters to obtain individual sensor-based state estimates which are then fused to obtain an improved joint state estimate. Whereas measurement fusion methods directly fuse the sensor measurements to obtain a weighted or combined measurement and then use a single Kalman filter to obtain the final state estimate based upon the fused observation. Measurement fusion methods generally provide better overall estimation performance, while state-vector fusion methods have a lower computation and communication cost and have the advantages of
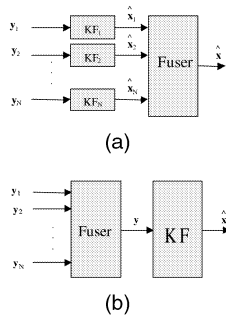
Fig. 1. Kalman-filter-based multisensor data fusion.
(a) State-vector fusion. (b) Measurement fusion.

parallel implementation and fault-tolerance [1, 2, 5]. It has also been pointed out [7, 10] that state-vector fusion methods are only effective when the Kalman filters are consistent, which restricts the practical applications of state-vector fusion methods. In many realistic applications such as navigation and target tracking, the underlying processes are often nonlinear, and the consequent Kalman filters are based on linearized process models (Jacobian linearization or neurofuzzy local linearization [11, 12]) and will usually be inconsistent due to the model errors introduced by the linearization process. Hence, when Kalman-filter-based multisensor data fusion is applied in these practical situations, measurement fusion is preferable to state-vector fusion.

There are two commonly used methods for measurement fusion. The first (Method I) simply merges the multisensor data [13, 14], which increases the dimension of the observation vector of the Kalman filter, and the second (Method II) combines the multisensor data based on minimum-mean-square-error estimates, keeping the observation vector dimension unchanged [5]. In comparative studies of state-vector fusion and measurement fusion conducted by Chang, et al. [2] and Roecker and McGillem [5], only the measurement fusion Method II was considered. Clearly, by making use of all the raw measurement information Method I should outperform Method II, but Method II has a lower computational load. Also, Method II may be inapplicable in some situations, such as with dissimilar sensors whose measurement matrices are of different sizes. It is natural to raise the following question: if Method II is applicable, under what conditions is its performance able to match that of Method I? Results on the theoretical analysis of the fused state estimate covariance matrices of the two measurement fusion methods are presented. In section II, it is shown that the two measurement fusion methods are functionally equivalent if the sensors, with different noise characteristics, have identical measurement matrices, as often happens in practical applications. If the sensors have identical measurement matrices, Method II is better than Method I due to its lower

computational cost, otherwise Method I is more flexible and more efficient. Also presented are some simulation results on state estimation using the two measurement fusion methods in Section III, to illustrate their comparative attributes.

II. THEORETICAL COMPARISON

Consider a dynamical target which is tracked by N sensors. The target dynamics and the sensors are modeled by the following discrete-time state-space model:

$$\mathbf{x}(t) = A(t)\mathbf{x}(t-1) + B(t)\mathbf{u}(t) + \mathbf{v}(t) \tag{1}$$

$$\mathbf{y}_j(t) = C_j(t)\mathbf{x}(t) + \mathbf{w}_j(t), \qquad j = 1,2,\ldots,N \tag{2}$$

where t represents the discrete-time index, $\mathbf{x}(t)$ is the state-vector, $\mathbf{u}(t)$ the input vector, $\mathbf{y}_j(t)$ measurement vectors, $\mathbf{v}(t)$ and $\mathbf{w}_j(t)$ zero-mean white Gaussian noise with covariance matrices $Q(t)$ and $R_j(t)$, respectively. It is assumed that the measurement noise is independent. By measurement fusion, the N sensor models can be integrated into the following single model:

$$\mathbf{y}(t) = C(t)\mathbf{x}(t) + \mathbf{w}(t) \tag{3}$$

where $\mathbf{w}(t) \sim N(\mathbf{0}, R(t))$. In this section, the two measurement fusion methods are formulated and their performance in state estimation are compared.

A. Measurement Fusion Method I

The measurement fusion Method I integrates the sensor measurement information by augmenting the observation vector as follows [13, 14]:

$$\mathbf{y}(t) = \mathbf{y}^{(\mathrm{I})}(t) = [\mathbf{y}_1(t) \quad \cdots \quad \mathbf{y}_N(t)]^T \tag{4}$$

$$C(t) = C^{(\mathrm{I})}(t) = [C_1(t) \quad \cdots \quad C_N(t)]^T \tag{5}$$

$$R(t) = R^{(\mathrm{I})}(t) = \mathrm{diag}[R_1(t) \quad \cdots \quad R_N(t)]. \tag{6}$$

B. Measurement Fusion Method II

The measurement fusion Method II obtains the fused measurement information by weighted observation as [5]:

$$\mathbf{y}(t) = \mathbf{y}^{(\mathrm{II})}(t) = \left[\sum_{j=1}^{N} R_j^{-1}(t)\right]^{-1} \sum_{j=1}^{N} R_j^{-1}(t)\mathbf{y}_j(t) \tag{7}$$

$$C(t) = C^{(\mathrm{II})}(t) = \left[\sum_{j=1}^{N} R_j^{-1}(t)\right]^{-1} \sum_{j=1}^{N} R_j^{-1}(t)C_j(t) \tag{8}$$

$$R(t) = R^{(\mathrm{II})}(t) = \left[\sum_{j=1}^{N} R_j^{-1}(t)\right]^{-1}. \tag{9}$$

C. The Kalman Filter and its Information Form

Given the state-space model described by (1) and (3), the Kalman filter provides an unbiased and optimal estimate of the state-vector in the sense of minimum estimate covariance, which can be described by the following equations [12–14].

Prediction:

$$\hat{\mathbf{x}}(t \mid t-1) = A(t)\hat{\mathbf{x}}(t-1 \mid t-1) + B(t)\mathbf{u}(t) \qquad (10)$$

$$P(t \mid t-1) = A(t)P(t-1 \mid t-1)A^T(t) + Q(t). \qquad (11)$$

Estimate (Correction):

$$K(t) = P(t \mid t-1)C^T(t)[C(t)P(t \mid t-1)C^T(t) + R(t)]^{-1} \qquad (12)$$

$$\hat{\mathbf{x}}(t \mid t) = \hat{\mathbf{x}}(t \mid t-1) + K(t)[\mathbf{y}(t) - C(t)\hat{\mathbf{x}}(t \mid t-1)] \qquad (13)$$

$$P(t \mid t) = [I - K(t)C(t)]P(t \mid t-1) \qquad (14)$$

where $\hat{\mathbf{x}}(t \mid t)$ represents the estimate of the state-vector $\mathbf{x}(t \mid t)$, $P(t \mid t)$ is the state estimate covariance matrix, and $K(t)$ is the Kalman gain matrix.

If we define a so-called information state vector: $\hat{\mathbf{z}}(t_1 \mid t_2) \equiv P^{-1}(t_1 \mid t_2)\hat{\mathbf{x}}(t_1 \mid t_2)$, where $P^{-1}(t_1 \mid t_2)$ is called the information matrix, then the standard Kalman filter can be transformed into the following information form.

Prediction:

$$\hat{\mathbf{z}}(t \mid t-1) = P^{-1}(t \mid t-1)A(t)P(t-1 \mid t-1)$$
$$\times \hat{\mathbf{z}}(t-1 \mid t-1) + P^{-1}(t \mid t-1)B(t)\mathbf{u}(t) \qquad (15)$$

$$P(t \mid t-1) = A(t)P(t-1 \mid t-1)A^T(t) + Q(t). \qquad (16)$$

Estimate (Correction):

$$\hat{\mathbf{z}}(t \mid t) = \hat{\mathbf{z}}(t \mid t-1) + C^T(t)R^{-1}(t)\mathbf{y}(t) \qquad (17)$$

$$P^{-1}(t \mid t) = P^{-1}(t \mid t-1) + C^T(t)R^{-1}(t)C(t). \qquad (18)$$

The information form of the Kalman filter, or information filter, is functionally equivalent to the Kalman filter, but has some computational advantages, especially in multisensor data fusion where the innovations covariance matrix $[C(t)P(t \mid t-1)C^T(t) + R(t)]$ is usually of high dimension and nondiagonal. The major difference between the standard Kalman filter and the information filter lies in their estimate phase. The estimate phase of the information filter is simpler as the gain matrix $K(t)$ in the standard Kalman filter is more complex than the term $C^T(t)R^{-1}(t)$ in the information filter, especially in multisensor data fusion where the inversion $[C(t)P(t \mid t-1)C^T(t) + R(t)]^{-1}$ in $K(t)$ may become computationally prohibitive.

D. On Functional Equivalence of the Two Measurement Fusion Methods

Comparing (4)–(6) with (7)–(9), we note that the treatment in the two measurement fusion methods are quite different. However, we find that there exists a certain form of functional equivalence between the two methods, contained in the following theorem.

THEOREM   *If the N sensors used for data fusion, with different and independent noise characteristics, have identical measurement matrices, i.e., $C_1(t) = C_2(t) = \cdots = C_N(t)$, then the measurement fusion Method I is functionally equivalent to the measurement fusion Method II.*

PROOF   The following formula in linear algebra will be used to cope with the inversion of matrices:

$$\begin{bmatrix} A_1 & A_2 \\ A_3 & A_4 \end{bmatrix}^{-1} = \begin{bmatrix} B_1 & B_2 \\ B_3 & B_4 \end{bmatrix} \qquad (19)$$

$$(A + HBH^T)^{-1} = A^{-1} - A^{-1}H(B^{-1} + H^T A^{-1}H)^{-1}H^T A^{-1} \qquad (20)$$

where $B_1 = (A_1 - A_2A_4^{-1}A_3)^{-1}$, $B_2 = -B_1A_2A_4^{-1}$, $B_3 = -A_4^{-1}A_3B_1$, and $B_4 = A_4^{-1} + A_4^{-1}A_3B_1A_2A_4^{-1}$.

If the standard Kalman filter is used, in order to demonstrate the functional equivalence of the two measurement fusion methods we only need to check whether the terms $K(t)C(t)$ and $K(t)\mathbf{y}(t)$ in Method I are functionally equivalent to those in Method II. Alternatively, if the information filter is used, then we need to check the functional equivalence between terms $C^T(t)R^{-1}(t)C(t)$ and $C^T(t)R^{-1}(t)\mathbf{y}(t)$ in both methods. To avoid confusion, the variables in Method I are indexed by $^{(I)}$ and the variables in Method II indexed by $^{(II)}$. For simplicity, the time argument in $C_j(t)$ and $R_j(t)$ will be omitted in the following derivation.

First, consider the case when the standard Kalman filter is applied. Because of the complexity of the innovations covariance matrix, direct derivation via this route is complex. Let us begin with sensor-to-sensor fusion, i.e., $N = 2$. Letting $C_1 = C_2 = C$ and $\Omega^{(I)} = CP^{(I)}(t \mid t-1)C^T$, we obtain the Kalman gain in Method I as follows:

$$K^{(I)}(t) = P^{(I)}(t \mid t-1)(C^{(II)})^T \begin{bmatrix} R_1 + \Omega^{(I)} & \Omega^{(I)} \\ \Omega^{(I)} & R_2 + \Omega^{(I)} \end{bmatrix}^{-1}$$
$$= P^{(I)}(t \mid t-1)C^T[(R_2 + \Omega^{(I)})^{-1}$$
$$\times R_2[R_1 + \Omega^{(I)} - \Omega^{(I)}(R_2 + \Omega^{(I)})^{-1}\Omega^{(I)}]^{-1},$$
$$\times (R_2 + \Omega^{(I)})^{-1} - (R_2 + \Omega^{(I)})^{-1}$$
$$\times R_2[R_1 + \Omega^{(I)} - \Omega^{(I)}(R_2 + \Omega^{(I)})^{-1}\Omega^{(I)}]^{-1}$$
$$\times \Omega^{(I)}(R_2 + \Omega^{(I)})^{-1}]. \qquad (21)$$

In Appendix A, the following equalities are proved:

$$(R_2 + \Omega^{(I)})^{-1} R_2 [R_1 + \Omega^{(I)} - \Omega^{(I)}(R_2 + \Omega^{(I)})^{-1}\Omega^{(I)}]^{-1}$$
$$= [\Omega^{(I)} + R_1(R_1 + R_2)^{-1}R_2]^{-1} R_2(R_1 + R_2)^{-1}$$

(22)

and

$$(R_2 + \Omega^{(I)})^{-1} - (R_2 + \Omega^{(I)})^{-1} R_2$$
$$\times [R_1 + \Omega^{(I)} - \Omega^{(I)}(R_2 + \Omega^{(I)})^{-1}\Omega^{(I)}]^{-1}\Omega^{(I)}(R_2 + \Omega^{(I)})^{-1}$$
$$= [\Omega^{(I)} + R_1(R_1 + R_2)^{-1}R_2]^{-1} R_1(R_1 + R_2)^{-1}.$$

(23)

Based on (21)–(23), we have

$$K^{(I)}(t) = P^{(I)}(t \mid t-1)C^T$$
$$\times [CP^{(I)}(t \mid t-1)C^T + R_1(R_1 + R_2)^{-1}R_2]^{-1}$$
$$\times [R_2(R_1 + R_2)^{-1}, \ R_1(R_1 + R_2)^{-1}]$$

(24)

$$K^{(I)}(t)C^{(I)}(t) = P^{(I)}(t \mid t-1)C^T$$
$$\times [CP^{(I)}(t \mid t-1)C^T + R_1(R_1 + R_2)^{-1}R_2]^{-1}C$$

(25)

$$K^{(I)}(t)\mathbf{y}^{(I)}(t) = P^{(I)}(t \mid t-1)C^T$$
$$\times [CP^{(I)}(t \mid t-1)C^T + R_1(R_1 + R_2)^{-1}R_2]^{-1}$$
$$\times [R_2(R_1 + R_2)^{-1}\mathbf{y}_1(t) + R_1(R_1 + R_2)^{-1}\mathbf{y}_2(t)].$$

(26)

If $C_1 = C_2 = C$, then $C^{(II)} = C$, and we obtain the Kalman gain in Method II as follows:

$$K^{(II)}(t) = P^{(II)}(t \mid t-1)C^T$$
$$\times [CP^{(II)}(t \mid t-1)C^T + R_1(R_1 + R_2)^{-1}R_2]^{-1}$$

(27)

and we can derive the terms $K^{(II)}(t)C^{(II)}(t)$ and $K^{(II)}(t)\mathbf{y}^{(II)}(t)$:

$$K^{(II)}(t)C^{(II)}(t) = P^{(II)}(t \mid t-1)C^T$$
$$\times [CP^{(II)}(t \mid t-1)C^T + R_1(R_1 + R_2)^{-1}R_2]^{-1}C$$

(28)

$$K^{(II)}(t)\mathbf{y}^{(II)}(t) = P^{(II)}(t \mid t-1)C^T$$
$$\times [CP^{(II)}(t \mid t-1)C^T + R_1(R_1 + R_2)^{-1}R_2]^{-1}$$
$$\times [R_2(R_1 + R_2)^{-1}\mathbf{y}_1(t) + R_1(R_1 + R_2)^{-1}\mathbf{y}_2(t)]$$

(29)

Note that (25) and (28) are in the same form and that (26) and (29) are also in the same form. Therefore, with the same initial conditions, i.e., $P^{(I)}(0 \mid 0) = P^{(II)}(0 \mid 0)$ and $\hat{\mathbf{x}}^{(I)}(0 \mid 0) = \hat{\mathbf{x}}^{(II)}(0 \mid 0)$, the Kalman filters based on the observation information generated by (4)–(6) and (7)–(9), irrespectively, will result in the same state estimate $\hat{\mathbf{x}}(t \mid t)$. This means that the two measurement fusion methods are functionally equivalent in the sensor-to-sensor case. This result can be generalized for N sensors. More conveniently, the generalized result can also be obtained based on the following proof with the information filter and the functional equivalence between the standard Kalman filter and information filter.

Now, consider the case when the information filter is applied. From (4)–(9), it is easy to prove the following equalities:

$$[C^{(I)}(t)]^T[R^{(I)}(t)]^{-1}C^{(I)}(t) = \sum_{j=1}^{N} C_j^T R_j^{-1} C_j$$

(30)

$$[C^{(I)}(t)]^T[R^{(I)}(t)]^{-1}\mathbf{y}^{(I)}(t) = \sum_{j=1}^{N} C_j^T R_j^{-1} \mathbf{y}_j$$

(31)

$$[C^{(II)}(t)]^T[R^{(II)}(t)]^{-1}C^{(II)}(t)$$
$$= \left[\left(\sum_{j=1}^{N} R_j^{-1}\right)^{-1} \sum_{j=1}^{N} R_j^{-1}C_j\right]^T \sum_{j=1}^{N} R_j^{-1}C_j$$

(32)

$$[C^{(II)}(t)]^T[R^{(II)}(t)]^{-1}\mathbf{y}^{(II)}(t)$$
$$= \left[\left(\sum_{j=1}^{N} R_j^{-1}\right)^{-1} \sum_{j=1}^{N} R_j^{-1}C_j\right]^T \sum_{j=1}^{N} R_j^{-1}\mathbf{y}_j.$$

(33)

If $C_j = C$, $j = 1, 2, \ldots, N$, then we have

$$[C^{(I)}(t)]^T[R^{(I)}(t)]^{-1}C^{(I)}(t) = [C^{(II)}(t)]^T[R^{(II)}(t)]^{-1}C^{(II)}(t)$$

(34)

$$[C^{(I)}(t)]^T[R^{(I)}(t)]^{-1}\mathbf{y}^{(I)}(t) = [C^{(II)}(t)]^T[R^{(II)}(t)]^{-1}\mathbf{y}^{(II)}(t)$$

(35)

Based on the formulation of the information filter (15)–(18), obviously there exists a functional equivalence between the two measurement fusion methods.

The functional equivalence of the two measurement fusion methods is limited to the case when $C_1 = C_2 = \cdots = C_N$. If $C_1 \neq C_2 \neq \cdots \neq C_N$, then the functional equivalence will no longer hold. Because Method I makes use of all the raw measurement information, it most likely provides a better estimate. Additionally, if the sensors are dissimilar, Method II may not work at all (e.g., if C_i and C_j are of different sizes). Based on the above theorem, we should choose Method II if $C_1 = C_2 = \cdots = C_N$ is satisfied, otherwise Method I is a better choice.

III. SIMULATION RESULTS

For experimental comparison of the two measurement fusion methods, simulation results are obtained in this section using the following target and

sensor models which are extensively studied in [1–8]:

$$\mathbf{x}(t) = \begin{bmatrix} 1 & T \\ 0 & 1 \end{bmatrix} \mathbf{x}(t-1) + \begin{bmatrix} T^2/2 \\ T \end{bmatrix} v(t) \qquad (36)$$

$$y_j(t) = C_j \mathbf{x}(t) + w_j(t), \qquad j = 1,2 \qquad (37)$$

where the sampling time $T = 1$, $v(t) = N(0,q)$, and $w_j(t) = N(0,R_j)$. In [1–8], simulation studies were carried out for comparing the fused state estimate covariance of the state-vector fusion method or the measurement fusion method with the single-sensor (unfused) state estimate covariance. In the first stage of our simulation studies, some results on the gain of the multisensor data fusion, which are similar to those reported in [1–8], are repeated. However, the simulation studies here are focused on the comparison of the fused state estimate covariance matrices of the two measurement fusion methods. Two cases are considered here. In case 1, two sensors have identical measurement matrices, which are set as $C_1 = C_2 = [1\ 0]$. In case 2, two sensors have different measurement matrices, which are set as $C_1 = [1\ 0]$ and $C_2 = [1\ 0.5]$. In both cases, two situations, i.e., $R_1 = R_2$ and $R_1 \neq R_2$, are considered.

The state-space model described by (36)–(37) satisfies the conditions under which the fused state estimate covariance $P(t\,|\,t)$ will converge to a steady-state value [7], which is denoted here by

$$\begin{bmatrix} P_{11} & P_{12} \\ P_{12} & P_{22} \end{bmatrix}.$$

Fig. 2 illustrates the results in case 1 with $R_1 = R_2 = 1$, where the fused state estimate covariances in steady-state values of the two measurement fusion methods are given with variation of the process noise covariance q from 0.001 to 1000. Curves of P_{11} versus q, P_{12} versus q, and P_{22} versus q are shown in Fig. 2(a), (b), and (c), respectively. The results from Method I are shown in solid lines and those from Method II in dashed lines. Similar results in case 1, with $R_1 = 1$ and $R_2 = 1.25$, are given in Fig. 3(a), (b), and (c) in the same format. From Figs. 2 and 3 we note that Method I and Method II obtain the same state estimation results, i.e., they are functionally equivalent as stated in the theorem. In a similar way, the results in case 2 are shown in Fig. 4 with $R_1 = R_2 = 1$ and in Fig. 5 with $R_1 = 1$ and $R_2 = 1.25$, respectively. Note that in case 2 the results from Method I and Method II are different, and Method I outperforms Method II. This is because Method I provides complete measurement information to the Kalman filter which actually has the ability of information integration by itself.

IV. CONCLUSION

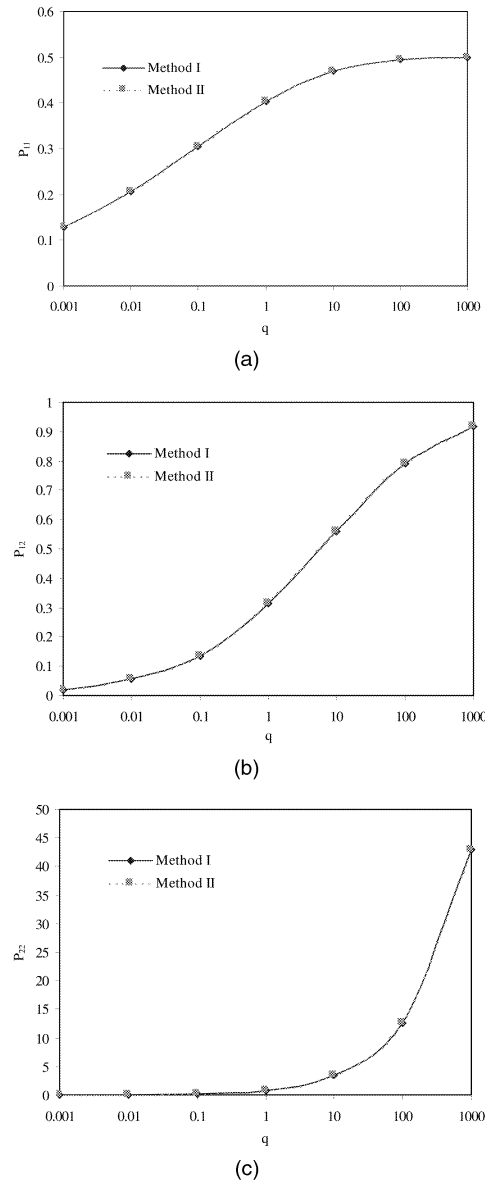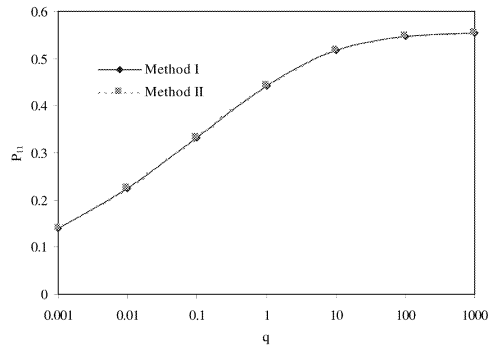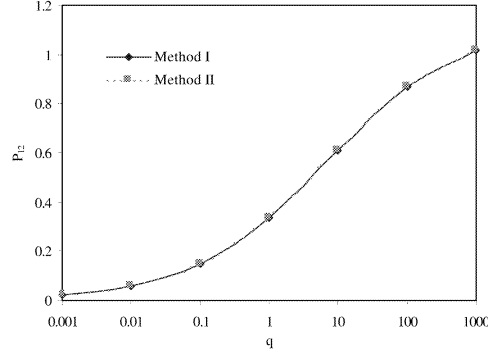This paper presents both theoretical and experimental results on the comparison of two

Fig. 2. Comparison of fused state estimate covariances of two measurement fusion methods in case 1 ($C_1 = C_2$), with $R_1 = R_2 = 1$. (a) P_{11} versus q. (b) P_{12} versus q. (c) P_{22} versus q.

measurement fusion methods for Kalman-filter-based multisensor data fusion. The two measurement fusion methods are functionally equivalent if the sensors have identical measurement matrices. In this case, Method II is more efficient than Method I, because of its lower computational cost. However, Method I outperforms Method II when the measurement matrices of the sensors are different. In addition, by comparatively examining the formulations of the two measurement fusion methods, we note that Method I is more flexible and will become more efficient in the sense of computational cost, when the number of sensors increases and the measurement matrices of sensors are different, and especially when the measurement matrices and noise characteristics are time-varying. Also, by using the information filter
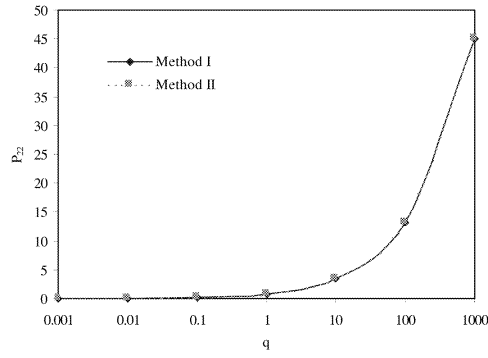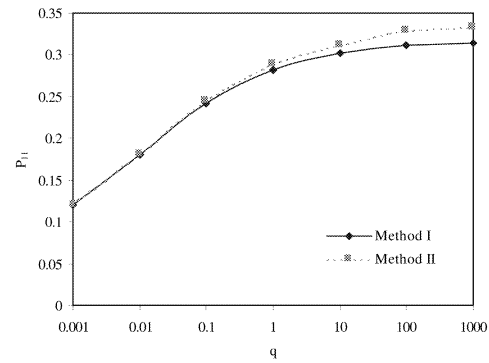
Fig. 3. Comparison of fused state estimate covariances of two measurement fusion methods in case 1 $(C_1 = C_2)$, $R_1 = 1$ and $R_2 = 1.25$. (a) P_{11} versus q. (b) P_{12} versus q. (c) P_{22} versus q.

Fig. 4. Comparison of fused state estimate covariances of two measurement fusion methods in case 2 $(C_1 \neq C_2)$, with $R_1 = R_2 = 1$. (a) P_{11} versus q. (b) P_{12} versus q. (c) P_{22} verus q.

the inverse of the high-dimensional innovations covariance matrix in Method I can be avoided. The above results would be very valuable in the design of practical multisensor data fusion systems for navigation and target tracking.
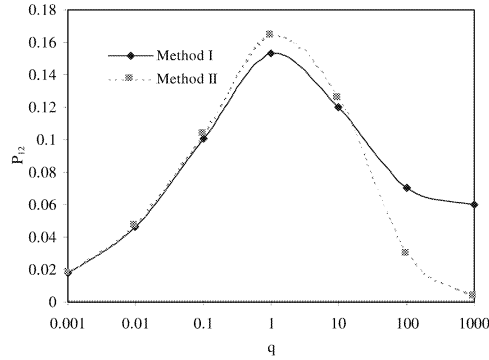
APPENDIX A: PROOF OF EQUATIONS (22) AND (23)

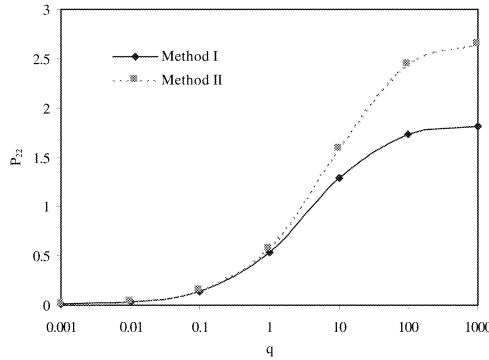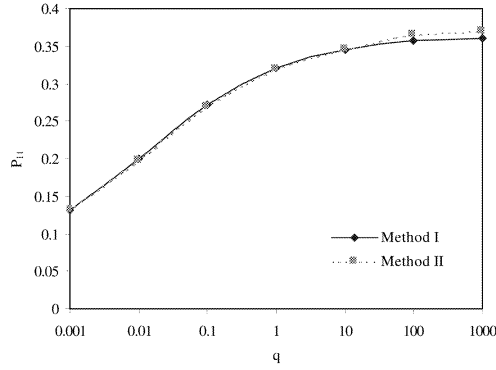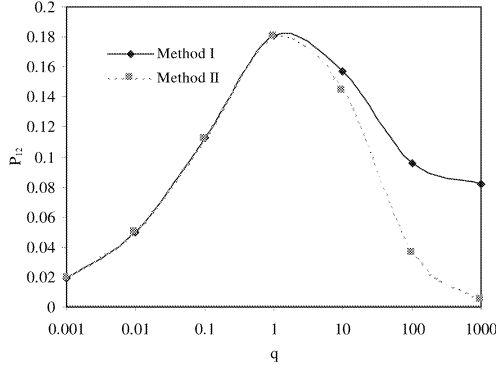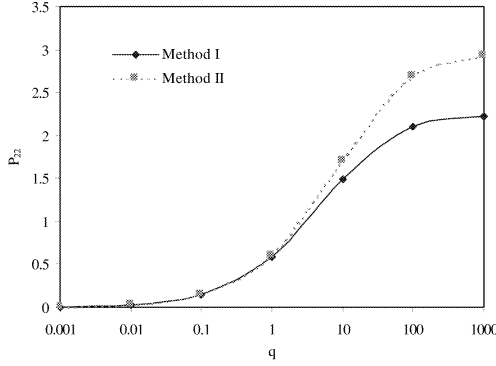Based on the matrix inversion lemma (20), (22) can be proved as follows:

$$(R_2 + \Omega^{(I)})^{-1} R_2 [R_1 + \Omega^{(I)} - \Omega^{(I)} (R_2 + \Omega^{(I)})^{-1} \Omega^{(I)}]^{-1}$$

$$= (R_2 + \Omega^{(I)})^{-1} R_2 [R_1 + \Omega^{(I)} (R_2 + \Omega^{(I)})^{-1} R_2]^{-1}$$

$$= (R_2 + \Omega^{(I)})^{-1} R_2 [(R_1 + R_2) - R_2 (R_2 + \Omega^{(I)})^{-1} R_2]^{-1}$$

$$= (R_2 + \Omega^{(I)})^{-1} R_2 [(R_1 + R_2) - R_2 (R_2 + \Omega^{(I)})^{-1} R_2]^{-1}$$

$$\times R_2 (R_2 + \Omega^{(I)})^{-1} (R_2 + \Omega^{(I)}) R_2^{-1}$$

$$= \{ [(R_2 + \Omega^{(I)}) - R_2 (R_1 + R_2)^{-1} R_2]^{-1}$$

$$- (R_2 + \Omega^{(I)})^{-1} \} \cdot (R_2 + \Omega^{(I)}) R_2^{-1}$$

$$= \{ [\Omega^{(I)} + R_1 (R_1 + R_2)^{-1} R_2]^{-1}$$

$$- (R_2 + \Omega^{(I)})^{-1} \} \cdot (R_2 + \Omega^{(I)}) R_2^{-1}$$

$$= [\Omega^{(I)} + R_1 (R_1 + R_2)^{-1} R_2]^{-1} (R_2 + \Omega^{(I)}) R_2^{-1} - R_2^{-1}$$

$$= [\Omega^{(I)} + R_1 (R_1 + R_2)^{-1} R_2]^{-1}$$

$$\times \{ (R_2 + \Omega^{(I)}) - [\Omega^{(I)} + R_1 (R_1 + R_2)^{-1} R_2] \} R_2^{-1}$$

$$= [\Omega^{(I)} + R_1 (R_1 + R_2)^{-1} R_2]^{-1} R_2 (R_1 + R_2)^{-1}. \qquad (38)$$

Fig. 5. Comparison of fused state estimate covariances of two measurement fusion methods in case 2 ($C_1 \neq C_2$), with $R_1 = 1$ and $R_2 = 1.25$. (a) P_{11} versus q. (b) P_{12} versus q. (c) P_{22} versus q.

Making use of the result in (38), we can prove (23) as follows:

$$(R_2 + \Omega^{(I)})^{-1} - (R_2 + \Omega^{(I)})^{-1} R_2$$

$$\times [R_1 + \Omega^{(I)} - \Omega^{(I)}(R_2 + \Omega^{(I)})^{-1}\Omega^{(I)}]^{-1} \cdot \Omega^{(I)}(R_2 + \Omega^{(I)})^{-1}$$

$$= (R_2 + \Omega^{(I)})^{-1} - [\Omega^{(I)} + R_1(R_1 + R_2)^{-1}R_2]^{-1} R_2$$

$$\times (R_1 + R_2)^{-1} \cdot \Omega^{(I)}(R_2 + \Omega^{(I)})^{-1}$$

$$= [\Omega^{(I)} + R_1(R_1 + R_2)^{-1}R_2]^{-1}$$

$$\times \{[\Omega^{(I)} + R_1(R_1 + R_2)^{-1}R_2] - R_2(R_1 + R_2)^{-1}\Omega^{(I)}\}$$

$$\times (R_2 + \Omega^{(I)})^{-1}$$

CORRESPONDENCE

$$= [\Omega^{(I)} + R_1(R_1 + R_2)^{-1}R_2]^{-1}$$

$$\times [R_1(R_1 + R_2)^{-1}R_2 + R_1(R_1 + R_2)^{-1}\Omega^{(I)}] \cdot (R_2 + \Omega^{(I)})^{-1}$$

$$= [\Omega^{(I)} + R_1(R_1 + R_2)^{-1}R_2]^{-1} \cdot R_1(R_1 + R_2)^{-1}$$

$$\times (R_2 + \Omega^{(I)})(R_2 + \Omega^{(I)})^{-1}$$

$$= [\Omega^{(I)} + R_1(R_1 + R_2)^{-1}R_2]^{-1} R_1(R_1 + R_2)^{-1}. \quad (39)$$

ACKNOWLEDGMENTS

The authors wish to thank Dr. Junbin Gao for valuable discussions.

QIANG GAN
CHRIS J. HARRIS
Image, Speech and Intelligent Systems Research Group
Department of Electronics and Computer Science
University of Southampton
Southampton SO17 1BJ
UK
E-mail: (qg@ecs.soton.ac.uk, cjh@ecs.soton.ac.uk)

REFERENCES

[1]   Chang, K. C., Tian, Z., and Saha, R. K. (1998)
      Performance evaluation of track fusion with information
      filter.
      In *Proceedings of International Conference on
      Multisource-Multisensor Information Fusion*, July 1998,
      648–655.

[2]   Chang, K. C., Saha, R. K., and Bar-Shalom, Y. (1997)
      On optimal track-to-track fusion.
      IEEE Transactions on Aerospace and Electronic Systems,
      33, 4 (1997), 1271–1276.

[3]   Saha, R. K., and Chang, K. C. (1998)
      An efficient algorithm for multisensor track fusion.
      IEEE Transactions on Aerospace and Electronic Systems,
      34, 1 (1998), 200–210.

[4]   Saha, R. K. (1996)
      Track-to-track fusion with dissimilar sensors.
      IEEE Transactions on Aerospace and Electronic Systems,
      32, 3 (1996), 1021–1029.

[5]   Roecker, J. A., and McGillem, C. D. (1988)
      Comparison of two-sensor tracking methods based on
      state vector fusion and measurement fusion.
      IEEE Transactions on Aerospace and Electronic Systems,
      24, 4 (1988), 447–449.

[6]   Bar-Shalom, Y., and Li, X. R. (1995)
      *Multitarget-Multisensor Tracking: Principles and
      Techniques.*
      Storrs, CT: YBS Publishing, 1995.

[7]   Bar-Shalom, Y., and Fortmann, T. E. (1988)
      Tracking and Data Association.
      New York: Academic Press, 1988.

[8]   Bar-Shalom, Y., and Campo, L. (1986)
      The effect of the common process noise on the
      two-sensor fused-track covariance.
      IEEE Transactions on Aerospace and Electronic Systems,
      22, 6 (1986), 803–805.

[9]   Bar-Shalom, Y. (1981)
      On the track-to-track correlation problem.
      IEEE Transactions on Automatic Control, **26**, 2 (1981),
      571–572.

[10] Mazor, E., Averbuch, A., Bar-Shalom, Y., and Dayan, J. (1998)
Interacting multiple model methods in target tracking: A survey.
IEEE Transactions on Aerospace and Electronic Systems, **34**, 1 (1998), 103–123.

[11] Gan, Q., and Harris, C. J. (1999)
Fuzzy local linearization and local basis function expansion in nonlinear system modeling.
IEEE Transactions on Systems, Man, and Cybernetics, **29**, Pt. B, 3 (1999).

[12] Gan, Q., and Harris, C. J. (1999)
Neurofuzzy state estimators using a modified ASMOD and Kalman filter algorithm.
In *Proceedings of International Conference on Computational Intelligence for Modelling Control and Automation*, Vienna, Feb. 1999, 214–219.

[13] Manyika, J., and Durrant-Whyte, H. (1994)
Data Fusion and Sensor Management: A Decentralized Information-Theoretic Approach.
New York: Ellis Horwood, 1994.

[14] Doyle, R. S., and Harris, C. J. (1996)
Multi-sensor data fusion for helicopter guidance using neuro-fuzzy estimation algorithms.
The Royal Aeronautical Society Journal (June/July 1996), 241–251.

A Coarse/Fine Search PN Code Acquisition Scheme

A parallel two-stage acquisition technique is described for direct sequence spread spectrum (DS/SS) range finding applications. The technique offers hardware complexity that scales better with code length than matched filter correlators while providing better performance than sequential detection using comparable hardware.

I. INTRODUCTION

The problem of code acquisition in direct sequence spread spectrum (DS/SS) systems has been studied extensively, and the basic compromise is between hardware complexity and acquisition time. Two basic search strategies, the matched filter correlator and the sequential detector, illustrate the extreme cases. The matched filter correlator approach is a hardware-intensive solution that quickly searches all of the possible code phases. The other extreme is a sequential detector in which a single active correlator tests each phase of the code serially until a match

is found. The sequential detector requires much less hardware but has a much longer acquisition time than the matched filter approach when long code sequences are used.

The coarse/fine (C/F) search approach presented here is a parallel two-stage acquisition technique. Other two-stage acquisition examples can be found in the literature [1–3]. These acquisition schemes were designed to reduce computational complexity. The C/F search scheme, however, was developed specifically to reduce the required hardware.

The specific application for the C/F approach is DS/SS range finding. This application requires rapid acquisition and code sequence synchronization in a channel that contains only the desired code sequence at the target modulation frequency. The repeating sequence contains L chips. A high signal-to-noise ratio (SNR) is expected for this application, and this high SNR is exploited to permit testing of several code phases in parallel during the initial acquisition search.

The storage required by an algorithm has a profound effect on the cost of the implementation hardware. One prior example [1] computes the L correlations of an m-sequence using a Walsh-Hadamard transform which reduces the computational complexity from L^2 additions to $(L + 1)\log_2(L + 1)$ additions. This method reduces computation significantly, but it requires storage for a full symbol of input samples.

The remainder of this paper first describes the C/F technique. Next, estimates of hardware complexity are provided for both the full symbol matched filter and the C/F approach. The C/F technique is shown to scale much better with code length than the full symbol matched filter. A performance estimate is provided for the C/F acquisition probability using a channel with additive white Gaussian noise (AWGN). Mean acquisition time estimates are offered for comparison between the C/F approach and a serial correlator made with comparable hardware complexity. The C/F technique is shown to work very well with the high SNR expected for the ranging application.

II. APPROACH

This approach is intended for ranging applications in which there is a large SNR. Further, this approach assumes that there are L chips per symbol with $L = 2^{2n} - 1$ and $n \in \aleph$. The C/F search consists of an initial coarse phase estimation followed by a fine phase calculation. The coarse estimation is accomplished using $\sqrt{L + 1}$ correlators to calculate correlations of smoothed input data for one symbol period (L chip periods). This is illustrated in Fig. 1. The input signal $r(t)$ is integrated over each chip period to form elements of the discrete sequence r_k